PHYSICAL REVIEW C VOLUME 23, NUMBER 5 MAY 1981

Relativistic effects in the Bethe-Brueckner theory of nuclear matter

M. R. Anastasio, L. S. Celenza, and C. M. Shakin
Department of Physics and Institute for Nuclear Theory, Brooklyn College of the City University of New York, Brooklyn, New York 11210
(Received 8 October 1980)

We extend the theory of nuclear matter to include a relativistic description of nucleon motion. In particular we allow for negative energy components in the nucleon wave function. The amplitude for these components is calculated using an extended version of the one-boson-exchange model of nuclear forces. We find that the inclusion of negative energy states (pair currents) provides a strongly density dependent repulsive interaction. (If one limits oneself to a description involving positive energy states only, this interaction appears as an effective repulsive many-body force.) Our extended theory leads to major modification of the saturation properties of nuclear matter. For example, a boson-exchange force which, in a standard calculation, leads to significant overbinding of nuclear matter at much too high a saturation density yields, in our relativistic analysis, quite good agreement with the generally accepted empirical values for the binding energy and density of nuclear matter. (This potential has strong tensor coupling for the ρ meson and a weak tensor force. These features are favored at this time on the basis of other theoretical considerations.) We conclude that, contrary to current thought, nuclear matter should be treated as a relativistic system.

[NUCLEAR STRUCTURE Relativistic effects in the saturation properties of nuclear matter.]

I. INTRODUCTION

Recently a good deal of effort has been expended in attempting to understand the nucleon-nucleon interaction on the basis of meson exchange processes. The simplest theory is the one-boson-exchange model of nuclear forces.[1] More complicated theories have also been considered. For example, several researchers have considered a much more detailed treatment of the two-pion-exchange contribution.[2] Further, there is an extensive body of work which is concerned with the role of the Δ isobar in intermediate states in the study of the NN system and nuclear matter.[3]

It is hoped that our increased knowledge of the nature of the nucleon-nucleon interaction will help us to understand the properties of finite nuclei and of nuclear matter. However, our understanding of these systems is still unsatisfactory.[4,5] In particular, it is found that if one makes a graph of the binding energy of nuclear matter (for various forces) as a function of the Fermi momentum, the results generally lie on a curve (the Coester band) which does not pass through the region containing the generally accepted empirical values.[5] It is worth noting that forces with relatively small tensor components lead to significant overbinding of nuclear matter at much too large a saturation density.[5] These forces, however, are favored at this time on the basis of other theoretical considerations.[6-8] For example, the force of Holinde and Machleidt[9] denoted as HM2 yields a binding energy per particle of about 23 MeV at a saturation point that corresponds to about *twice* the empirical density. However, this force has large tensor ρ coupling which is considered to be correct at this time.[8] When compared to interactions with stronger tensor forces, HM2 yields an improved fit to the forward proton production in deuteron photodisintegration.[7]

In general it does not appear possible to explain the properties of nuclear matter or finite nuclei using currently available theories. (Note that while the consideration of three-body cluster terms in the case of the Reid potential can yield a reasonable result for the properties of nuclear matter,[5] the results for finite nuclei are still quite unsatisfactory.[10])

On the whole, relativistic effects have been considered to be small corrections and only a few studies have been made dealing with such effects. The studies that have been made have been concerned more with kinematical effects rather than dynamical features. In this work, however, we will show that relativistic effects can be very large. These effects are strongly density dependent and make major modifications in the saturation curve. In particular, for those forces that saturate at too high a density, the modification of the results due to relativistic effects can be quite dramatic.

Since our calculations are novel we should explain our point of view in some detail. We will only consider potentials in which the nucleon-nucleon interaction is derived from some version of the boson-exchange model since coordinate space potentials do not lend themselves to a relativistic treatment. Let us consider the simplest kind of meson exchange interaction, the so-called one-boson-exchange model, for simplicity. In this case

the nucleon-nucleon interaction is obtained from the solution of a relativistic two-body problem.[1] For example, one may start from a Bethe-Salpeter equation,

$$M = K + KG_F M \,, \tag{1.1}$$

where G_F is a Feynman propagator for the intermediate state nucleons. One can rewrite this equation as two equations,

$$M = U + UgM \,, \tag{1.2}$$

$$U = K + K(G_F - g)U \,. \tag{1.3}$$

Here g is a propagator that has the same right-hand cut as G_F. The propagator g contains a delta function which reduces the four-dimensional equation to a three-dimensional equation.[1] Usually g contains projection operators $\Lambda_+(\vec{k})$ which project onto the space of positive energy spinors. There are many possible choices for g; however, for each choice made one can determine a relativistic *quasipotential* U. Various quasipotentials have been determined by fitting the two-nucleon scattering data using the one-boson exchange model of nuclear forces.[1] We will investigate the properties of nuclear matter using several of these quasipotentials.

We now write Eq. (1.2) as

$$M = U + Ug^{++}M \,, \tag{1.4}$$

where we have put $g = g^{++}$ as a reminder that both intermediate state particles are represented by positive-energy spinors.[1,2] For the study of the two-nucleon scattering amplitude we may write Eq. (1.4) as

$$M^{++++} = U^{++++} + U^{++++}g^{++}M^{++++} \,, \tag{1.5}$$

where

$$\langle \vec{p}s_1, \vec{q}s_2 | M^{++++} | \vec{p}'s_1', \vec{q}'s_2' \rangle$$

$$\equiv \langle \bar{u}^{(s_1)}(\vec{p})\bar{u}^{(s_2)}(\vec{q}) | M | u^{(s_1')}(\vec{p}')u^{(s_2')}(\vec{q}') \rangle \,, \tag{1.6}$$

etc. Equation (1.5) has been studied extensively and the quasipotential U^{++++} has been parametrized in terms of coupling constants, masses, and form factors for various exchanged mesons[1,2,4] ($\pi, \rho, \omega, \sigma, \delta, \eta, \phi, \ldots$).

Application of the one-boson-exchange interaction in the study of nuclear matter requires some further analysis. For example, one replaces g^{++} by $\hat{g}^{++}$, where $\hat{g}^{++}$ is taken to include dispersive effects and Pauli principle restrictions. Thus one considers the solution of the equation

$$\hat{M}^{++++} = U^{++++} + U^{++++}\hat{g}^{++}\hat{M}^{++++} \,, \tag{1.7}$$

where $\hat{M}$ is the effective interaction in the medium (usually called the reaction matrix). In Eq. (1.7) we have neglected medium effects on the kernel U^{++++}. Once one has obtained the solution of Eq. (1.7) one may calculate the binding energy of the system. For example, one may write for the potential energy

$$\mathcal{E}_{\rm pot} = \tfrac{1}{2} \sum_{ss'} \int \frac{d\vec{p}}{(2\pi)^3} \frac{d\vec{q}}{(2\pi)^3} \frac{m}{E(\vec{p})} \frac{m}{E(\vec{q})} \langle \bar{u}^{(s)}(\vec{p})\bar{u}^{(s')}(\vec{q}) | \hat{M}(1 - P_{12}) | u^{(s)}(\vec{p})u^{(s')}(\vec{q}) \rangle \tag{1.8}$$

$$= \tfrac{1}{2} \sum_{ss'} \int \frac{d\vec{p}}{(2\pi)^3} \frac{d\vec{q}}{(2\pi)^3} \langle \vec{p}s, \vec{q}s' | G(\epsilon_{\vec{p}} + \epsilon_{\vec{q}}) | \vec{p}s, \vec{q}s' \rangle_A \,. \tag{1.9}$$

In going from Eq. (1.8) to Eq. (1.9) we have introduced a somewhat more familiar notation for the reaction matrix of the Bethe-Brueckner theory of nuclear matter.[11] (Note that we are suppressing explicit reference to the isospin quantum numbers.) In Eq. (1.9) the inclusion of the energy argument in the reaction matrix is a reminder that this quantity is calculated self-consistently. Correspondingly the s value for the evaluation of $\hat{M}$ is given by $s^2 = (p^0 + q^0)^2 - (\vec{q} + \vec{p})^2$. The relationship between p^0 and $\epsilon_{\vec{p}}$ is $p^0 = m + \epsilon_{\vec{p}}$, etc.

For further reference it is useful to indicate the calculation of Eq. (1.8) in a diagrammatic fashion. (See Fig. 1.) In Fig. 1(a) the small circles denote vertex functions. This diagram is calculated with the massive systems of A, $A-1$, or $A-2$ particles kept on the mass shells. (Some further details concerning the use of such vertex functions for finite systems are given in Refs. 12 and 13.)

We are now in a position to consider in more detail the nature of the approximation being used when one writes Eq. (1.8). Basically one is using wave functions for the particles in the Fermi sea that are plane waves multiplied by *positive energy* Dirac spinors. We recall [with reference to Fig. 1(a) and Ref. 12] that the product of the vertex function and the nucleon propagator is proportional to the matrix element of the nucleon field operator taken between two many-particle states. For example, let the nuclear matter state of A particles (more precisely, baryon number equal to A) with total momentum zero be denoted as $|\vec{0}\rangle$. Further, consider the state with baryon number $(A-1)$ of momentum $-\vec{p}$ and spin projection $-s$: $|-\vec{p}, -s\rangle$. The matrix element of the nucleon field operator taken between these states may be written as[12]

$$\langle -\vec{p}-s|\Psi(0)|\vec{0}\rangle=\frac{1}{(2\pi)^{3/2}}\left[\frac{m}{E(\vec{p})}\right]^{1/2}[a_s(\vec{p})u^{(s)}(\vec{p})+(-1)^{1/2-s}b(\vec{p})v^{(-s)}(-\vec{p})] \tag{1.10}$$

$$=\frac{1}{(2\pi)^{3/2}}\left[\frac{m}{E(\vec{p})}\right]^{1/2}[a(\vec{p})u^{(s)}(\vec{p})+(-1)^{1/2-s}b(\vec{p})w^{(s)}(\vec{p})], \tag{1.11}$$

where *we have restricted* $\vec{p}$ *to be along the z axis* and where we have defined $w^{(s)}(\vec{p})\equiv v^{(-s)}(-\vec{p})$. (We normalize such that $a^2+b^2=1$.) Now it is clear that the approximation being used to obtain Eq. (1.8) from the evaluation of Fig. 1(a) is given by setting $a(\vec{p})=1$ and $b(\vec{p})=0$. It can be seen that this is not a consistent approximation.

Let us define the amplitude $\phi_s(\vec{p})$:

$$\phi_s(\vec{p})=\langle -\vec{p},-s|\Psi(0)|\vec{0}\rangle(2\pi)^{3/2} \tag{1.12}$$

$$=\left[\frac{m}{E(\vec{p})}\right]^{1/2}[a_s(\vec{p})u^{(s)}(\vec{p})+(-1)^{1/2-s}b(\vec{p})w^{(s)}(\vec{p})]. \tag{1.13}$$

This amplitude satisfies the Dirac equation

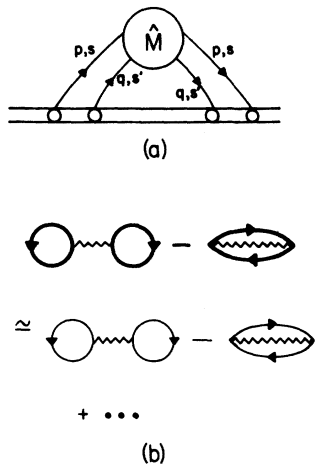

FIG. 1. (a) Schematic representation of the potential energy calculation by means of a Feynman diagram. Here the small circles are vertex functions and the single lines represent Feynman propagators for off-mass-shell nucleons. Further, $\hat{M}_{ex}=\hat{M}(1-P_{12})$ is an antisymmetrized two-nucleon scattering amplitude modified for Pauli principle and dispersive effects. (See Ref. 13 for a discussion of the use of such diagrams in Hartree-Fock theory. Reference 12 contains some discussion of vertex functions, propagators, and wave functions in a relativistic theory of finite nuclei.) (b) Goldstone diagrams representing the direct and exchange contributions to the potential energy. Here the heavy lines denote a *self-consistent* relativistic wave function and the wavy line denotes the reaction matrix. If one limits oneself to an expansion of the wave functions using only positive energy spinors (light lines), one obtains the standard expression for the potential energy. [See Eqs. (1.8) and (1.9).]

$$[\gamma\cdot p-m-\Sigma(p)]\phi_s(p)=0. \tag{1.14}$$

Here $\Sigma(p)$ is the self-energy operator. [More precisely, $\Sigma(p)$ is the difference of the nucleon self-energy in the medium and in the vacuum. This quantity is zero if the density of the nuclear matter is zero.] Now as long as $\Sigma(p)\neq 0$, the specification $a(\vec{p})=1$ and $b(\vec{p})=0$ does not yield a solution of Eq. (1.14).

In this work we investigate the consequences for the theory of nuclear matter which follow from a detailed calculation of the solution of Eq. (1.14). *As we will see, the inclusion of the negative energy states in Eqs. (1.12) and (1.13) leads to major modifications in the calculated properties of nuclear matter.* These effects may be considered as arising from the use of a self-consistent wave function in a relativistic Bethe-Brueckner theory. (We recall that there is no self-consistency consideration for the wave function in the nonrelativistic theory of nuclear matter.) The reader desiring a detailed derivation of the relativistic model used in this work is invited to read the paper immediately preceding this one in this journal.

II. CALCULATION OF THE NUCLEON SELF-ENERGY OPERATOR

Since we have made an expansion of the wave function in terms of the spinors $u^{(s)}(\vec{p})$ and $w^{(s)}(\vec{p})$ [Eq. (1.13)], it is useful to determine the matrix elements of the self-energy operator in the same basis. Again *restricting p to be along the z axis*, we define[14]

$$\Sigma^{++}_{ss'}(p)=\delta_{ss'}\bar{u}^{(s)}(\vec{p})\Sigma(p)u^{(s)}(\vec{p})=\delta_{ss'}\Sigma^{++}(p), \tag{2.1}$$

$$\Sigma^{-+}_{ss'}(p)=\delta_{ss'}\bar{w}^{(s)}(\vec{p})\Sigma(p)u^{(s')}(\vec{p})=\delta_{ss'}(-1)^{1/2-s}\Sigma^{-+}(p), \tag{2.2}$$

$$\Sigma^{+-}_{ss'}(p)=\delta_{ss'}\bar{u}^{(s)}(\vec{p})\Sigma(p)w^{(s')}(\vec{p})=\delta_{ss'}(-1)^{1/2-s}\Sigma^{+-}(p), \tag{2.3}$$

$$\Sigma^{--}_{ss'}(p)=\delta_{ss'}\bar{w}^{(s)}(\vec{p})\Sigma(p)w^{(s')}(\vec{p})=\delta_{ss'}\Sigma^{--}(p). \tag{2.4}$$

One can show that $\Sigma^{-+}_{ss}(p)=\Sigma^{+-}_{ss}(p)$ and that $\Sigma^{-+}_{ss}=-\Sigma^{-+}_{-s-s}(p)$. Further, the solution of Eq. (1.14) yields a relation $p^0=p^0(\vec{p})$, so that we can define

$\Sigma(\vec{p}) \equiv \Sigma[p^0(\vec{p}), \vec{p}]$, etc. We note that $\Sigma^{-+}(\vec{p})$ is proportional to $|\vec{p}|$ for small $|\vec{p}|$.

From Eq. (1.14) we find the coupled equations[14]

$$[p^0 - E(\vec{p})]a = \frac{m}{E(\vec{p})}(\Sigma^{++}a + \Sigma^{+-}b), \tag{2.5}$$

$$[p^0 + E(\vec{p})]b = \frac{m}{E(\vec{p})}(\Sigma^{--}b + \Sigma^{-+}a). \tag{2.6}$$

From these equations we have

$$\alpha(\vec{p}) = \frac{b(\vec{p})}{a(\vec{p})} = \frac{m}{E(\vec{p})}\left\{\frac{\Sigma^{-+}(|\vec{p}|)}{p^0 + E(\vec{p}) - [m/E(\vec{p})]\Sigma^{--}(|\vec{p}|)}\right\} \tag{2.7}$$

$$\simeq [m/E(\vec{p})]\Sigma^{-+}(|\vec{p}|)/[m + E(\vec{p})], \tag{2.8}$$

where in Eq. (2.8) we have put $p^0 \simeq m$ and neglected $\Sigma^{--}(\vec{p})$ with respect to $m + E(\vec{p})$.

Models for the calculation of $\Sigma^{-+}(\vec{p})$ and $\Sigma^{++}(\vec{p})$ have been discussed extensively in earlier works.[14,15] We have defined

$$\Sigma^{++}(p) = \sum_{s'} \int \frac{d\vec{q}}{(2\pi)^3} \frac{m}{E(\vec{q})} \langle \bar{u}^{(s)}(\vec{p}) \bar{u}^{(s')}(\vec{q}) | \hat{M}^{++++}(1 - P_{12}) | u^{(s)}(\vec{p}) u^{(s')}(\vec{q}) \rangle, \tag{2.9}$$

$$\Sigma^{-+}(p) = \sum_{s'} \int \frac{d\vec{q}}{(2\pi)^3} \frac{m}{E(\vec{q})} \langle \bar{w}^{(1/2)}(\vec{p}) \bar{u}^{(s')}(\vec{q}) | \hat{M}^{-+++}(1 - P_{12}) | u^{(1/2)}(\vec{p}) u^{(s')}(\vec{q}) \rangle, \tag{2.10}$$

and

$$\Sigma^{--}(p) = \sum_{s'} \int \frac{d\vec{q}}{(2\pi)^3} \frac{m}{E(\vec{q})} \langle \bar{w}^{(s)}(\vec{p}) \bar{u}^{(s')}(\vec{q}) | \hat{M}^{-+-+}(1 - P_{12}) | w^{(s)}(\vec{p}) u^{(s')}(\vec{q}) \rangle. \tag{2.11}$$

Note that $\Sigma^{++}_{ss}(p)$ and $\Sigma^{--}_{ss}(p)$ are independent of s. We should remark that the Σ^{++}, Σ^{-+}, and Σ^{--} defined in Eqs. (2.9)–(2.11) are only the *leading terms* in an approximation to the fundamental quantities defined in Eqs. (2.1)–(2.4). The quantities Σ^{++} and Σ^{-+} should be calculated using the exact (self-consistent) density matrix for the system. In Eqs. (2.9)–(2.11) we have approximated this density matrix in terms of positive energy spinors only. This approximation is adequate for our purposes in this work. We propose to do a fully self-consistent calculation at a future time; however, we do not expect any significant changes in our results for the saturation curves presented in Sec. VIII.

We have calculated $\hat{M}^{-+++}$ using the following equation based on Eq. (1.4):

$$\hat{M}^{-+++} = U^{-+++} + U^{-+++}\hat{g}^{++}\hat{M}^{++++} \tag{2.12}$$

$$= U^{-+++}(1 + \hat{g}^{++}\hat{M}^{++++}) \tag{2.13}$$

$$= U^{-+++}\hat{\Omega}^{++++}. \tag{2.14}$$

We note that while Eq. (2.14) is obtained without approximation it has the appearance of a relativistic distorted wave approximation for $\hat{M}^{-+++}$.[14] Some results of our calculations of $\Sigma^{++}(\vec{p})$, $\Sigma^{-+}(\vec{p})$, and $\Sigma^{--}(\vec{p})$ will be presented in Secs. III–V.

In these calculations pseudovector coupling is used for the pion-nucleon vertex. As noted in our previous work[14] $\Sigma^{-+}(\vec{p})$ is larger than might be expected since the various mesons add *coherently* in the construction of $\Sigma^{-+}(\vec{p})$. The knowledge of this quantity enables us to construct $\alpha(\vec{p})$ using Eq. (2.8). To order $\alpha^2(\vec{p})$ we may write

$$\phi_s(\vec{p}) = \left[\frac{m}{E(\vec{p})}\right]^{1/2}\left\{\left[1 - \frac{\alpha^2}{2}(\vec{p})\right]u^{(s)}(\vec{p}) + (-1)^{1/2-s}\alpha(\vec{p})w^{(s)}(\vec{p})\right\} \tag{2.15}$$

and thus with $u^{(s)\dagger}(\vec{p})u^{(s)}(\vec{p}) = w^{(s)\dagger}(\vec{p})w^{(s)}(\vec{p}) = E(\vec{p})/m$, we have

$$\phi_s^\dagger(\vec{p})\phi_s(\vec{p}) = 1. \tag{2.16}$$

The generalization of Eq. (2.15) for $\vec{p}$ in an arbitrary direction is

$$\phi_s(\vec{p}) = \left[\frac{m}{E(\vec{p})}\right]^{1/2}\left\{\left[1 - \frac{\alpha^2(\vec{p})}{2}\right]u^{(s)}(\vec{p}) + \alpha(\vec{p})\sum_{s'}\langle s'|\vec{\sigma}\cdot\hat{\vec{p}}|s\rangle w^{(s')}(\vec{p})\right\}. \tag{2.17}$$

Since $\langle s|\sigma_z|s'\rangle = \delta_{ss'}(-1)^{1/2-s}$, Eq. (2.17) reduces to Eq. (2.15) for $\vec{p} = p\hat{z}$.

In Secs. VI and VII we describe the modifications of the kinetic energy and potential energy when we replace

$$\phi_s^{(0)}(\vec{p}) = \left[\frac{m}{E(\vec{p})}\right]^{1/2} u^{(s)}(\vec{p}) \tag{2.18}$$

by $\phi_s(\vec{p})$ given in Eqs. (2.15) and (2.17).

III. CALCULATION OF $\Sigma^{++}(|\vec{p}|)$

In this section we present results for our calculation of $\Sigma^{++}(|\vec{p}|)$ defined in Eq. (2.9). We consider the one-boson-exchange potentials of Ref. 9(HM2) and of Ref. 17 (HEA).

In Fig. 2 we show Σ^{++} as a function of $|\vec{p}|/k_F$ for

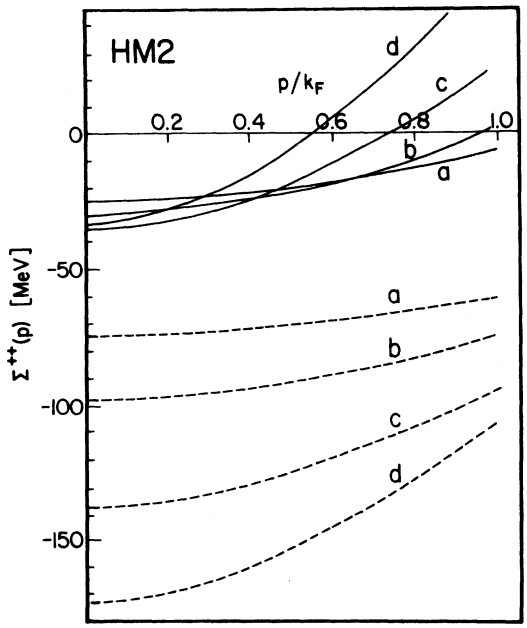

FIG. 2. The quantity $\Sigma^{++}(\vec{p})$ as a function of $|\vec{p}|/k_F$. The various curves represent calculations performed for different values of k_F. The solid lines represent the values of $\Sigma^{++}(\vec{p})$ obtained in the Hartree-Fock approximation ($M=U$) and the dashed curves are the results obtained including correlation effects [Eq. (2.9)]. These results indicate that correlation corrections make major modifications in $\Sigma^{++}(\vec{p})$. These calculations are made using the interaction of Ref. 9 (HM2). (a) $k_F=1.2$ fm^{-1}, (b) $k_F=1.36$ fm^{-1}, (c) $k_F=1.6$ fm^{-1}, and (d) $k_F=1.8$ fm^{-1}.

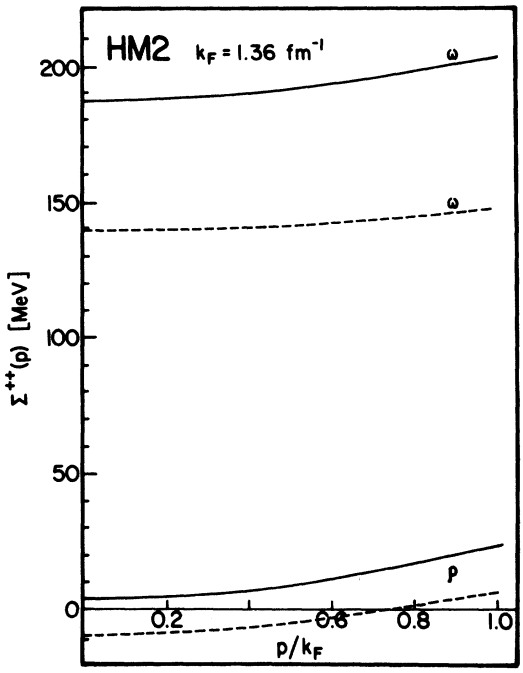

FIG. 3. Contributions to $\Sigma^{++}(|\vec{p}|)$ due to the exchange the ω and ρ mesons for the potential HM2. The solid lines denote the contributions in the Hartree-Fock approximation. The dashed curve shows the results of including correlations. [See Eqs. (3.1)–(3.5).]

various values of k_F for the potential HM2. The solid lines represent the values of Σ^{++} obtained in the Hartree-Fock approximation ($\hat{M}=U$) and the dashed curves are the results including correlation effects. (It is clear that the Hartree-Fock approximation is inadequate.) In Figs. 3 and 4 we present the contributions to Σ^{++} due to the exchange of individual mesons. Again the solid lines denote the results based upon the Hartree-Fock approximation and the dashed lines are the results including correlation effects. One may write for the quasipotential

$$U=\sum_{i=1}^{N}U_i=U_\pi+U_\sigma+U_\omega+\cdots, \tag{3.1}$$

where U_i is the potential corresponding to the exchange of a particular meson. We also note that

$$\hat{M}^{++++}=\sum_{i=1}^{N}U_i^{++++}(1+\hat{g}^{++}\hat{M}^{++++}) \tag{3.2}$$

$$=\sum_{i=1}^{N}\hat{M}_i^{++++}, \tag{3.3}$$

where

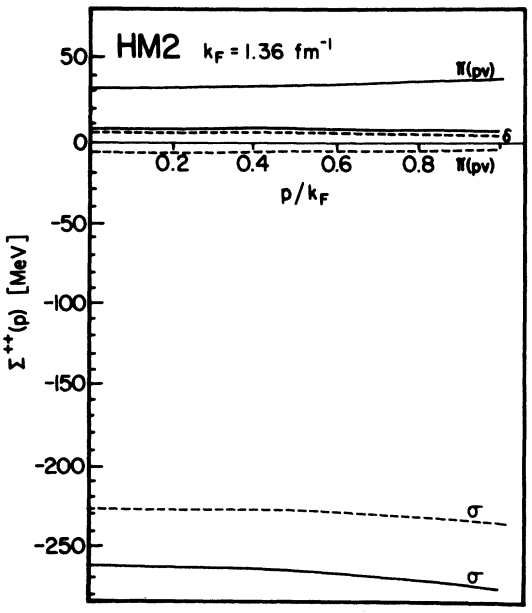

FIG. 4. Contributions to $\Sigma^{++}(|\vec{p}|)$ due to the exchange of σ, π, and δ mesons for the potential HM2. (See caption to Fig. 3.)

$$\hat{M}_i^{++++} = U_i^{++++}(1 + \hat{g}^{++}\hat{M}^{++++}) . \qquad (3.4)$$

The Hartree-Fock results for Σ^{++} shown as the solid lines in Figs. 3 and 4 result from the approximation $\hat{M}_i^{++++} = U_i^{++++}$. The results for Σ^{++} shown as dashed lines result from the use of the $\hat{M}_i^{++++}$ of Eq. (3.4) in Eq. (2.9). Note that in both cases

$$\Sigma^{++}(\vec{p}) = \sum_{i=1}^{N} \Sigma_i^{++}(\vec{p}) , \qquad (3.5)$$

where Σ_i^{++} is the self-energy obtained from the use of $\hat{M}_i^{++++}$ in Eq. (2.9). [See Eq. (3.3).]

In Figs. 5–7 we present corresponding results for $\Sigma^{++}(|\vec{p}|)$ and $\Sigma_i^{++}(|\vec{p}|)$ for the potential HEA.[17] One interesting feature of these results is the behavior of the pion contribution as seen in Figs. 4 and 7. In the Hartree-Fock approximation one has a repulsive contribution to $\Sigma^{++}(|\vec{p}|)$ of about 30 MeV; however, in the presence of correlations the pion contribution becomes small for HM2 (Fig. 4) and *strongly attractive* for HEA (Fig. 7). This feature has its origins in the presence of *tensor correlations*. (The effect is much stronger for HEA since HEA has a stronger tensor force than HM2.) To some degree therefore, the pion contribution to Σ^{++}, when calculated in the presence of correlations, is similar to that of the σ meson. Note, however, that the dependence of this contribution on $|\vec{p}|$ is different for the pion and the σ meson. (See Fig. 7, for example.)

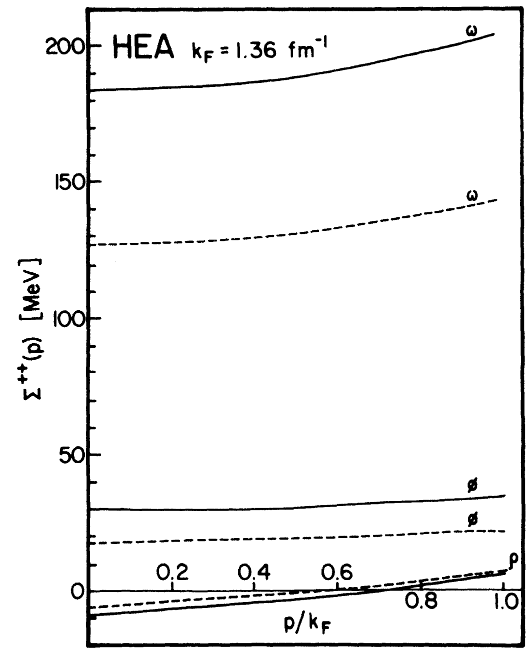

FIG. 6. Contributions to $\Sigma^{++}(|\vec{p}|)$ due to the exchange of ω, ϕ, and ρ mesons for the potential HEA. (See caption to Fig. 3.)

IV. CALCULATION OF $\Sigma^{-+}(|\vec{p}|)$

In this section we present results for our calculations of $\Sigma^{-+}(|\vec{p}|) = \Sigma^{-+}_{1/2\,1/2}(|\vec{p}|)$ defined in Eq. (2.10). In Fig. 8 we present our values

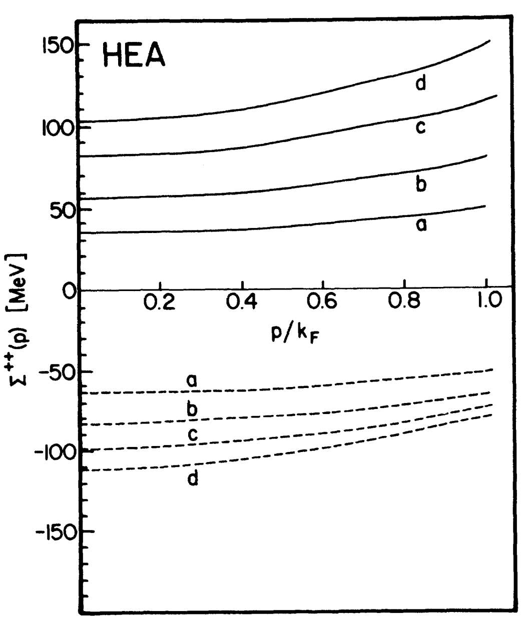

FIG. 5. Same caption as Fig. 2 except that the interaction is HEA (Ref. 17). (a) $k_F = 1.2$ fm^{-1}, (b) $k_F = 1.36$ fm^{-1}, (c) $k_F = 1.5$ fm^{-1}, and (d) $k_F = 1.6$ fm^{-1}.

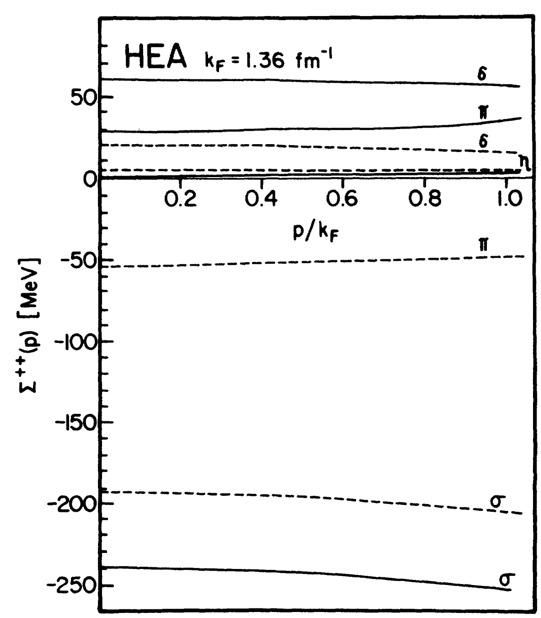

FIG. 7. Contributions to $\Sigma^{++}(|\vec{p}|)$ due to the exchange of σ, π, δ, and η mesons for the potential HEA. (See caption to Fig. 3.)

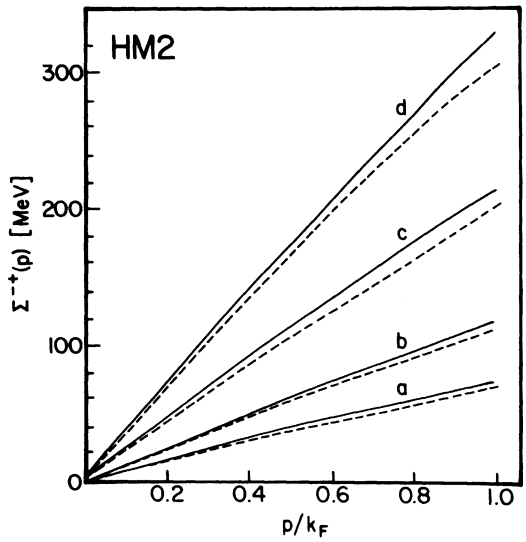

FIG. 8. Calculated values of $\Sigma^{-+}_{1/2\,1/2}(\vec{p})$ for the interaction of Ref. 9 (HM2). The various curves represent calculations made for various values of k_F. The solid lined denote the results for calculations carried out in a Hartree-Fock approximation, i.e., $M^{-+++}=U^{-+++}$. The dashed lines are the results obtained after correlation effects are included. [See Eqs. (2.11)–(2.13).]. We note that in contrast to the results for $\Sigma^{++}(\vec{p})$, correlation effects are rather unimportant in the calculation of $\Sigma^{-+}(\vec{p})$. (a) k_F=1.2 fm^{-1}, (b) k_F=1.36 fm^{-1}, (c) k_F=1.6 fm^{-1}, and (d) k_F=1.8 fm^{-1}.

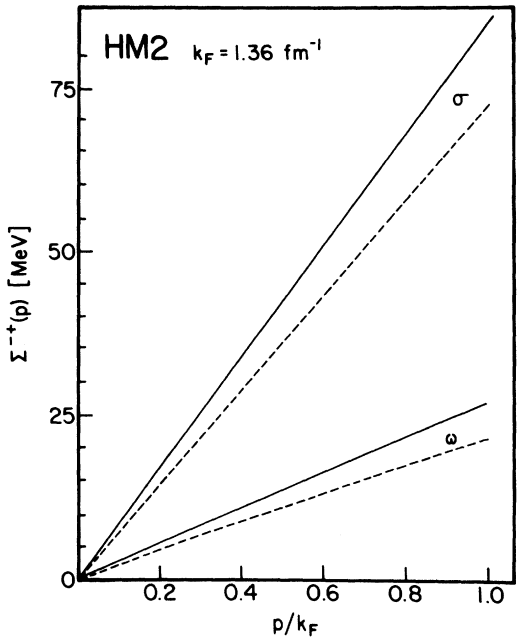

FIG. 9. Contributions to $\Sigma^{-+}(|\vec{p}|)$ from the exchange of σ and ω mesons for the interaction HM2. (See caption to Fig. 8.)

for $\Sigma^{-+}_{1/2\,1/2}(|\vec{p}|)$ calculated using the interaction HM2 in the Hartree-Fock approximation (solid line). The results including the effects of correlations are shown as the dashed lines. The effect of including correlations is remarkably small. In Figs. 9 and 10 we present the contributions of the individual mesons to the calculation of $\Sigma^{-+}(|\vec{p}|)$ for HM2. We remark that the exchange of the σ meson makes the major contribution to $\Sigma^{-+}(|\vec{p}|)$. This aspect of the theory clearly requires further investigation since the σ meson (often called the ϵ meson) is not an established resonance such as the ρ and ω mesons. It is, however, an essential feature of any pseudopotential constructed in the one-boson exchange model of nuclear forces.

In Figs. 11-13 we present values for $\Sigma^{-+}(|\vec{p}|)$ calculated with the interaction HEA. The results shown in Figs. 8 and 11 are remarkably similar. [Calculations for another one-boson-exchange potential, which we will denote as HM3′, also give very similar results for $\Sigma^{-+}(|\vec{p}|)$.] From the calculations we have made thus far we would conclude that $\Sigma^{-+}(|\vec{p}|)$ is largely *potential independent* and also largely independent of correlation effects. (See Figs. 8 and 11.) Again we can remark upon the interesting behavior of the pion contribution as seen in Figs. 10 and 13. In both cases correlations *enhance* the pion contribution to $\Sigma^{-+}(|\vec{p}|)$ changing a negative contribution to one close to zero (Fig. 10) for HM2 and to a positive contribution for HEA (Fig. 13).

It is also of interest to note that for both HEA

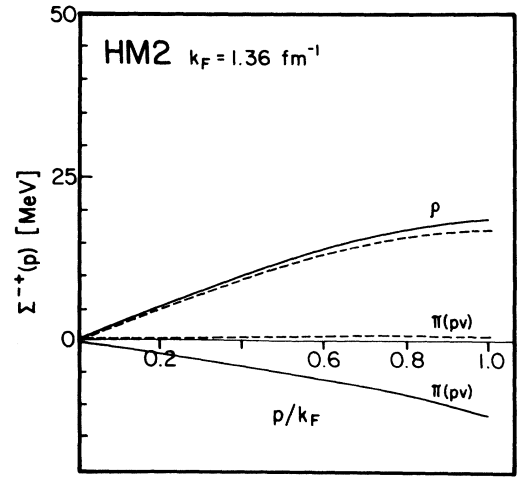

FIG. 10. Contributions to $\Sigma^{-+}(|\vec{p}|)$ from the exchange of π and ρ mesons for the interaction HM2. Pseudovector coupling is used for πNN vertex. (See caption to Fig. 8.)

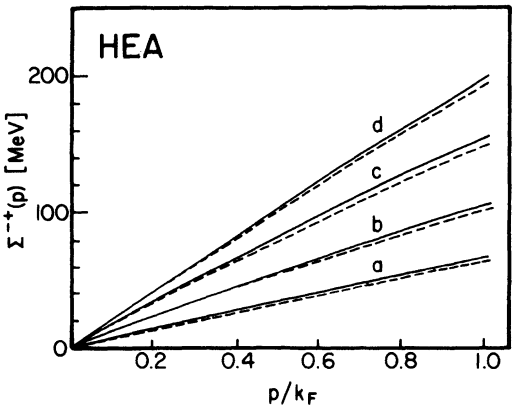

FIG. 11. Calculated values of $\Sigma^{-+}_{I/2\,1/2}(|\vec{p}|)$ for the interaction HEA. (See caption to Fig. 8.) (a) k_F=1.2 fm^{-1}, (b) k_F=1.36 fm^{-1}, (c) k_F=1.5 fm^{-1}, and (d) k_F=1.6 fm^{-1}.

and HM2, the contributions of the σ and ω mesons calculated in the Hartree-Fock approximation add to a value quite similar to that obtained from the sum of *all* meson contributions when correlation effects are included. Therefore a theory which contains *only* a σ and ω meson can yield a good value for Σ^{+-} in the Hartree-Fock approximation. (The value obtained for Σ^{+-} in a $\sigma+\omega$ model is also satisfactory if the Hartree approximation is used.)

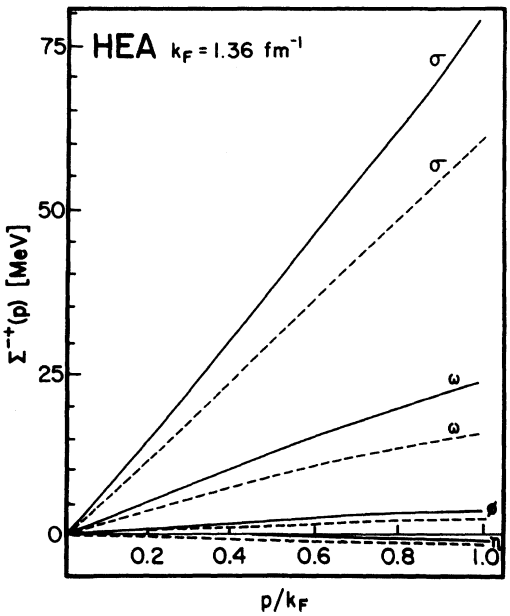

FIG. 12. Contributions to $\Sigma^{-+}_{I/2\,1/2}(|\vec{p}|)$ due to the exchange of σ, ω, ϕ, and η mesons for the potential HEA. (See caption to Fig. 8.)

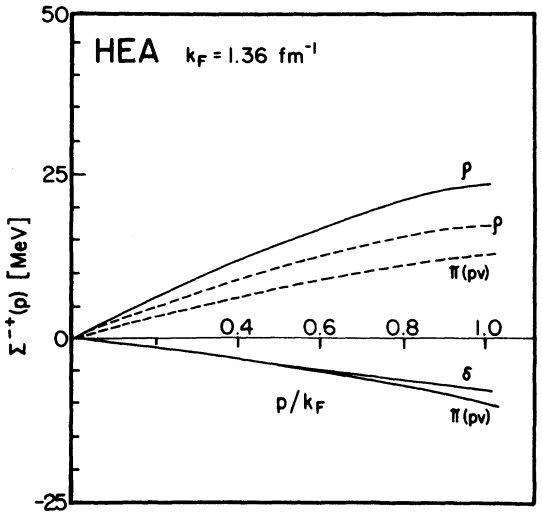

FIG. 13. Contributions to $\Sigma^{-+}_{I/2\,1/2}(|\vec{p}|)$ due to the exchange of the ρ, π, and δ mesons. The contribution of the δ meson in the presence of correlations is negligible. (See caption to Fig. 8.)

V. CALCULATION OF $\Sigma^{--}(|\vec{p}|)$

In Figs. 14-17 we present the results of our calculations for Σ^{--}. Again the solid lines denote the Hartree-Fock results and the dashed lines represent the results when correlation effects

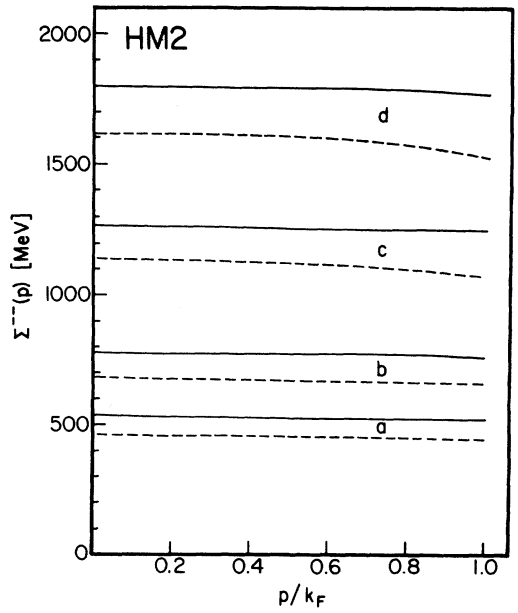

FIG. 14. Calculated values of $\Sigma^{--}(|\vec{p}|)$ for the potential HM2. The solid lines represent results obtained in the Hartree-Fock approximation and the dashed lines represent the results when correlations are included. (a) k_F=1.2 fm^{-1}, (b) k_F=1.36 fm^{-1}, (c) k_F=1.6 fm^{-1}, and (d) k_F=1.8 fm^{-1}.

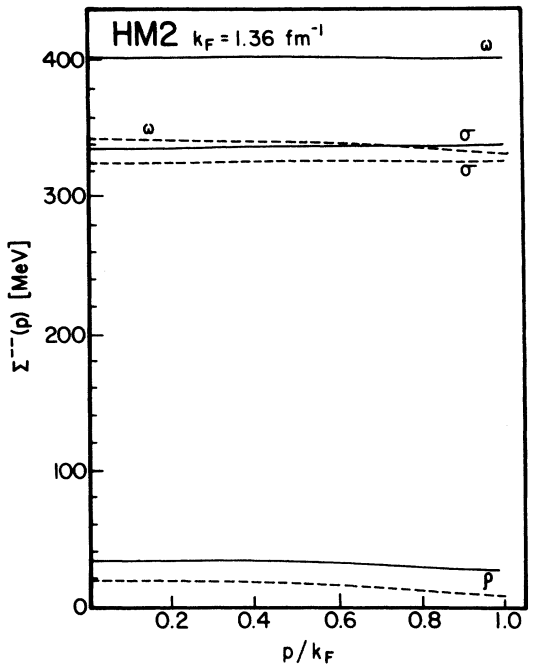

FIG. 15. Contributions of the individual meson to the calculation of $\Sigma^{--}(|\vec{p}|)$ in the Hartree-Fock approximation for the potential HM2 are shown as the solid lines. The dashed lines represent the results when correlations are included.

are included. We note that Σ^{--} is quite large since, unlike the case of Σ^{++}, the σ and ω contributions add coherently. Correlation effects are significant but not very large. For example,

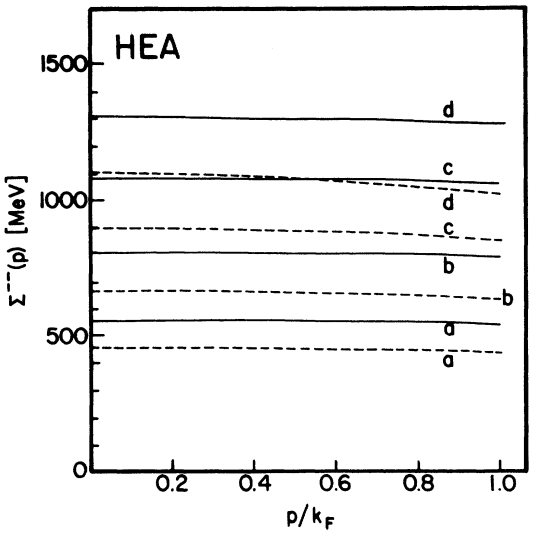

FIG. 16. Calculated values of $\Sigma^{--}(|\vec{p}|)$ for the potential HEA. The solid lines represent results obtained in the Hartree-Fock approximation and the dashed lines represent the results when correlations are included. (a) $k_F = 1.2$ fm^{-1}, (b) $k_F = 1.36$ fm^{-1}, (c) $k_F = 1.5$ fm^{-1}, and (d) $k_F = 1.6$ fm^{-1},

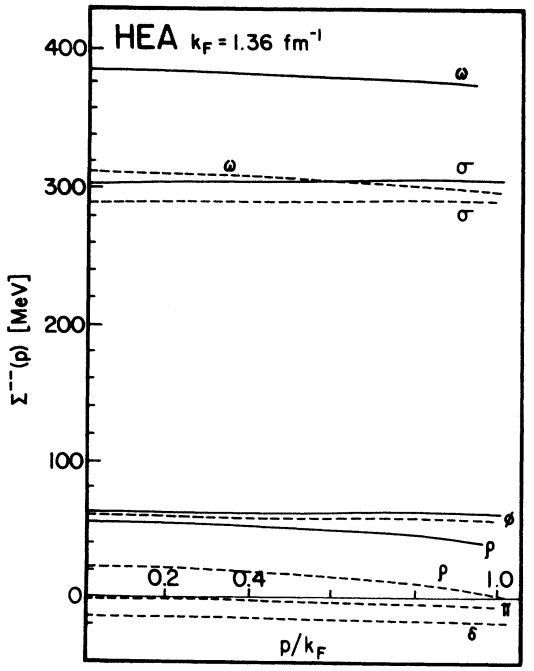

FIG. 17. Contributions of the individual mesons to the calculation of $\Sigma^{--}(|\vec{p}|)$ in the Hartree-Fock approximation for the potential HEA are shown as the solid lines. The dashed lines represent the results when correlations are included.

these effects reduce the value of $\Sigma^{--}(0)$ from 810 to 670 MeV for the potential HEA. (See Fig. 16.) Further, mesons other than the σ and ω make only a relatively small contribution to Σ^{--}.

The contributions of the individual mesons in the calculation of Σ^{--} are shown in Fig. 15(HM2) and Fig. 17 (HEA). The contributions of the π, η, and δ mesons are negligible for the potential HM2 and therefore these contributions are not indicated in Fig. 15. Similarly the contribution of the η meson, and the (Hartree-Fock) contributions of the π and δ mesons are not shown in Fig. 17.

VI. MODIFICATION OF THE KINETIC ENERGY

As a simple exercise we can show that the density of the system is unchanged if we use $\phi_s(\vec{p})$ rather than $\phi_s^{(0)}(\vec{p})$. The density operator is

$$n(\vec{x}) = \sum_s \bar{\Psi}_s(\vec{x})\gamma^0\Psi_s(\vec{x}) . \tag{6.1}$$

If the ground state of our nuclear matter system of momentum $\vec{W}$ is denoted as $|\vec{W}\rangle$ with $\langle\vec{W}|\vec{W}'\rangle = \delta(\vec{W}-\vec{W}')$, we have for the matrix element of the number operator

$$\langle \vec{W}' | N_{op} | \vec{0} \rangle = \langle \vec{W}' | \int d\vec{x}\, n(\vec{x}) | \vec{0} \rangle$$
$$= \sum_s \int\int d\vec{x} \langle \vec{W}' | \Psi_s^\dagger(\vec{x}) | -\vec{p} - s \rangle d\vec{p}$$
$$\times \langle -\vec{p}, -s | \Psi_s(\vec{x}) | \vec{0} \rangle . \quad (6.2)$$

Using

$$\Psi(\vec{x}) = e^{i\vec{P}\cdot\vec{x}} \Psi(\vec{0}) e^{-i\vec{P}\cdot\vec{x}} \quad (6.3)$$

we have

$$\langle \vec{W}' | N_{op} | \vec{0} \rangle = (2\pi)^3 \delta(\vec{W}') \sum_s \int d\vec{p} \langle \vec{W}' | \Psi^\dagger(\vec{0}) | -\vec{p} - s \rangle$$
$$\times \langle -\vec{p} - s | \Psi(\vec{0}) | \vec{0} \rangle$$
$$= \delta(\vec{W}') \sum_s \int d\vec{p}\, \phi_s^\dagger(\vec{p}) \phi_s(\vec{p})$$
$$= \delta(\vec{W}') \sum_s \int d\vec{p} . \quad (6.4)$$

The effective volume is $(2\pi)^3$ so that the density is

$$\rho = \sum_s \int \frac{d\vec{p}}{(2\pi)^3} = \frac{2}{3\pi^2} k_F^3 , \quad (6.5)$$

where we have used a statistical factor of 4 for each state of momentum $\vec{p}$.

With this elementary calculation completed we can go on to calculate the modification of the kinetic energy when $\phi_s^{(0)}(\vec{p})$ is replaced by $\phi_s(\vec{p})$. We write

$$H_0 = \int d\vec{x} \Psi^\dagger(\vec{x}) \left(\vec{\alpha} \cdot \frac{1}{i} \vec{\nabla} + \gamma^0 m \right) \Psi(\vec{x}) . \quad (6.6)$$

Again making use of Eq. (6.3) we find

$$\langle \vec{W}' | H_0 | \vec{0} \rangle = \delta(\vec{W}') \int d\vec{p}\, \bar{\phi}_s(\vec{p}) (\vec{\gamma} \cdot \vec{p} + m) \phi_s(\vec{p}) . \quad (6.7)$$

We note that in the preceding paper we obtained an expression for the total energy of the system [Eq. (10.5) of that work] ,

$$E = \sum_s \int \frac{d\vec{p}}{(2\pi)^3} \frac{m}{E(\vec{p})} \bar{f}^{(s)}(\vec{p}) (\vec{\gamma} \cdot \vec{p} + m) f^{(s)}(\vec{p})$$
$$+ \tfrac{1}{2} \sum_{ss'} \int \frac{d\vec{p}}{(2\pi)^3} \frac{d\vec{q}}{(2\pi)^3} \frac{m}{E(\vec{p})} \frac{m}{E(\vec{q})}$$
$$\times \langle \bar{f}^{(s)}(\vec{p}) \bar{f}^{(s')}(\vec{q}) | \hat{M}(1 - P_{12}) | f^{(s)}(\vec{p}) f^{(s')}(\vec{q}) \rangle , \quad (6.8)$$

where the $f^{(s)}(\vec{p})$ are related to the $\phi_s(\vec{p})$ used here by $\phi_s(\vec{p}) = [m/E(\vec{p})]^{1/2} f^{(s)}(\vec{p})$. [See Eq. (2.17).] In the foregoing analysis we have presented an alternative derivation of the first term of Eq. (6.8), the energy of the Dirac field.

We are using the Bjorken-Drell[16] conventions so that our spinors satisfy

$$(\vec{\gamma} \cdot \vec{p} + m) u^{(s)}(\vec{p}) = \gamma^0 E(\vec{p}) u^{(s)}(\vec{p}) , \quad (6.9)$$

$$(\vec{\gamma} \cdot \vec{p} + m) w^{(s)}(\vec{p}) = -\gamma^0 E(\vec{p}) w^{(s)}(\vec{p}) . \quad (6.10)$$

Therefore using Eq. (2.17) we find that the kinetic energy per particle is

$$\frac{\mathcal{E}_{kin}}{A} = \frac{3}{k_F^3} \int_0^{k_F} p^2 dp \{ [E(\vec{p}) - m] - \alpha^2(\vec{p}) [2E(\vec{p})] \} . \quad (6.11)$$

Of course if $\alpha = 0$ and $[E(\vec{p}) - m] \simeq p^2/2m$, we obtain $\mathcal{E}_{kin}/A = \frac{3}{5}[k_F^2/2m]$, the standard nonrelativistic result. Further, we remark that one-half of the correction term in Eq. (6.11) arises from the α^2 term in $a(\vec{p})$. Thus we see that it is vital to maintain the correct normalization of the $\phi_s(\vec{p})$. [See Eqs. (2.15) and (2.16) and Fig. 18.]

In Fig. 19 we present the kinetic energy per particle as a function of k_F. The dashed line is the result for $\alpha = 0$ and the solid line represents Eq. (6.11). We note that the relativistic correction to the kinetic energy, which is about 17% at $k_F = 1.36$ fm^{-1}, grows extremely rapidly with increasing density. We remark that at the higher densities it is more appropriate to call the quantity given by Eq. (6.11) and represented in Fig. 19, the "Dirac energy" since it has little resemblence to the nonrelativistic or relativistic kinetic energy of a noninteracting system.

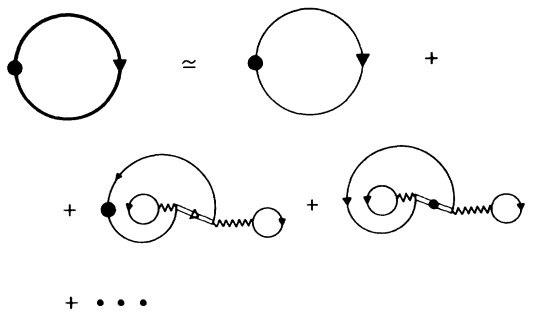

FIG. 18. Representation of the kinetic energy by Goldstone diagrams. The wavy line is a reaction matrix and the black dot is the kinetic energy operator. The heavy line denotes the self-consistent relativistic wave function. Double down going lines denote negative energy states. Single light lines denote states represented by positive energy spinors only.

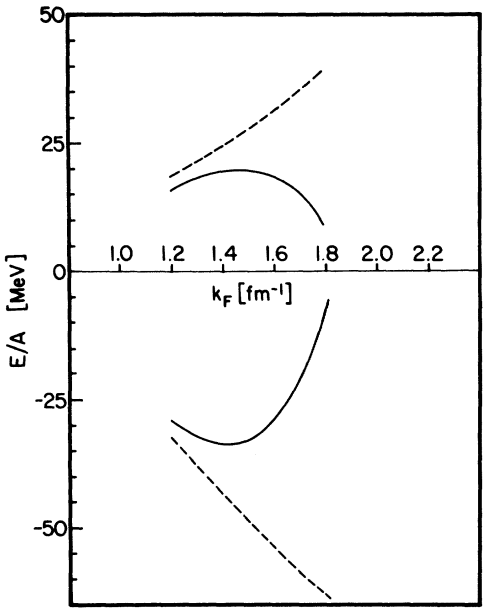

FIG. 19. Representation of the kinetic energy and potential energy versus k_F for the potential HM2. Results obtained with the standard expression for the kinetic energy are shown in the upper half of the figure as a dashed line. The solid line is the result for this quantity when the relativistic correction is included [Eq. (6.10)]. The corresponding curves for the potential energy are shown in the lower portion of the figure.

VII. MODIFICATION OF THE POTENTIAL ENERGY

The modification of the potential energy may be obtained from Eq. (1.8) by replacing $u^{(s)}$ by $[au^{(s)} + (-1)^{1/2-s}bw^{(s)}]$, i.e., replacing $\phi_s^{(0)}(\vec{p})$ by $\phi_s(\vec{p})$. [See Eq. (2.15).] This leads to a correction to the potential energy per particle of the form

$$\Delta\left(\frac{\mathcal{E}_{\rm pot}}{A}\right)=\frac{3}{k_F{}^3}\int_0^{k_F} p^2dp\,\alpha^2(\vec{p})\left[4m-\frac{2m}{E(\vec{p})}\,\Sigma^{--}(|\vec{p}|)\right] \tag{7.1}$$

if we use Eq. (2.7). In writing Eq. (7.1) we have dropped quite small terms of the order $\Sigma^{++}(\vec{p})/4m$. If we also neglect terms of the order $\Sigma^{--}(\vec{p})/2m$ we have

$$\Delta\left(\frac{\mathcal{E}_{\rm pot}}{A}\right)=\frac{3}{k_F{}^3}\int_0^{k_F} p^2dp\,\alpha^2(\vec{p})(4m)\,, \tag{7.2}$$

where the use of Eq. (2.8) is implied. Combining Eq. (7.2) with Eq. (3.10) we have for the *total correction*

$$\Delta\left(\frac{\mathcal{E}_{\rm kin}+\mathcal{E}_{\rm pot}}{A}\right)=\frac{3}{k_F{}^3}\int_0^{k_F} p^2dp\,\alpha^2(\vec{p})[4m-2E(\vec{p})]$$

$$\simeq (2m)\left(\frac{3}{k_F{}^3}\right)\int_0^{k_F} p^2dp\,\alpha^2(\vec{p})\,. \tag{7.3}$$

We refer to Fig. 20 for a diagrammatic representation of the nature of these corrections to the potential energy.

VIII. MODIFICATION OF THE SATURATION CURVE FOR NUCLEAR MATTER

In this section we will present results of our calculations for the potential of Ref. 9 (HM2) and for the potential of Ref. 17 (HEA). We will concentrate most of our discussion on the potential HM2.

In Fig. 8 we presented some results for $\Sigma^{++}_{1/2\,1/2}(\vec{p})$ for HM2. The calculations were made for various values of k_F and therefore we can discuss the dependence of Σ^{++} on k_F or on the density. Therefore we will write $\Sigma^{++}_{ss}(\vec{p},k_F)$ or $\Sigma^{++}_{ss}(\vec{p},\rho)$ in this section. We can make a simple approximation to the results shown in Fig. 3:

$$\Sigma^{++}_{1/2\,1/2}(\vec{p},k_F)=\frac{|\vec{p}|}{k_F}\left(\frac{k_F}{1.36}\right)^{3.6}(110)\ \text{MeV}\,, \tag{8.1}$$

where k_F is to be expressed in units of fm^{-1}. Equation (8.1) expresses the (approximate) linear dependence of $\Sigma^{++}_{ss}(\vec{p},k_F)$ on $|\vec{p}|$. Using Eq. (8.1) we see that a reasonable approximation for $\alpha^2(\vec{p})$ is

$$[\alpha(\vec{p},k_F)]^2=\left(\frac{110}{2m}\right)^2\left(\frac{|\vec{p}|}{k_F}\right)^2\left(\frac{k_F}{1.36}\right)^{7.2} \tag{8.2}$$

$$=\left(\frac{110}{2m}\right)^2\left(\frac{|\vec{p}|}{k_F}\right)^2\left(\frac{\rho}{\rho_0}\right)^{2.4}. \tag{8.3}$$

In Eq. (8.2) we have made the k_F dependence of $\alpha^2(\vec{p})$ explicit and introduced ρ_0, the density corresponding to $k_F=1.36$ fm^{-1}. The quantity $2m$ in Eqs. (8.2) and (8.3) should be expressed in MeV units.

Let us write the relativistic correction of Eq. (7.3) as

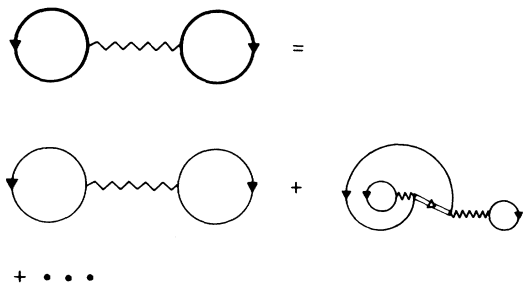

FIG. 20. Representation of relativistic corrections to the potential energy. The heavy lines denote self-consistent relativistic wave functions. The wavy lines are reaction matrices. The double lines are negative energy states and the single lines are occupied states (hole states) represented by positive energy spinors.

$$\Delta E \simeq \frac{3}{k_F^3} \int_0^{k_F} p^2 dp\, \alpha^2(\vec{p}, k_F)(2m). \tag{8.4}$$

Inserting the approximation given in Eq. (5.3) in this expression we find $\Delta E \simeq 3.86(k_F/1.36)^{7.2}$. A more accurate calculation yields

$$\Delta E = (3.6 \text{ MeV}) \left(\frac{k_F}{1.36}\right)^{7.2} \tag{8.5}$$

$$= (3.6 \text{ MeV}) \left(\frac{\rho}{\rho_0}\right)^{2.4}. \tag{8.6}$$

From these simple considerations we see that the relativistic correction is strongly density dependent. Further insight can be gained by inspection of Fig. 19 which presents the results of computations for the potential HM2. In the upper half of this figure we present the standard calculation of the kinetic energy (dashed line) and the calculation which includes the relativistic correction [Eq. (6.10)]. We remark that the relativistic correction is about 17% at $k_F = 1.36$ fm^{-1} and rapidly becomes quite large as the density increases. We have, approximately, $\Delta[\mathcal{E}_{\text{kin}}/A] \simeq -3.6 \text{ MeV}(\rho/\rho_0)^{2.4}$. In the lower half of Fig. 19 we show the standard calculation for the potential energy for the interaction HM2 (dashed line). Inclusion of the relativistic correction yields the solid line. This relativistic correction is given to a good approximation by $\Delta[\mathcal{E}_{\text{pot}}/A] \simeq 7.2 \text{ MeV}(\rho/\rho_0)^{2.4}$ and represents about a 20% correction at $k_F = 1.36$ fm^{-1}.

It is interesting to note that for HM2 the dependence of the potential energy (dashed curve) on k_F is almost linear in the region $1.2 \text{ fm}^{-1} \lesssim k_F \lesssim 1.8 \text{ fm}^{-1}$. In this region we may write $\mathcal{E}_{\text{pot}}/A \simeq -12 \text{ MeV} - 28.7 \text{ MeV}\,(\rho/\rho_0)^{1/3}$. Therefore combining our results we have approximately, for $1.2 \text{ fm}^{-1} \leq k_F \leq 1.8 \text{ fm}^{-1}$ only,

$$\left(\frac{E}{A}\right)_{\text{Rel}} \simeq \left[22.9\left(\frac{\rho}{\rho_0}\right)^{2/3} - 12 - 28.7\left(\frac{\rho}{\rho_0}\right)^{1/3} + 3.6\left(\frac{\rho}{\rho_0}\right)^{2.4}\right](\text{MeV}). \tag{8.7}$$

(We recall that ρ_0 is the density corresponding to $k_F = 1.36$ fm^{-1}.) The standard nonrelativistic approximation is obtained by dropping the last term in Eq. (8.7),

$$\left(\frac{E}{A}\right)_{\text{NR}} \simeq \left[22.9\left(\frac{\rho}{\rho_0}\right)^{2/3} - 12 - 28.7\left(\frac{\rho}{\rho_0}\right)^{1/3}\right](\text{MeV}). \tag{8.8}$$

The approximate expressions given in Eqs. (8.7) and (8.8) are for the interaction HM2. The results of exact calculations for HM2 and HEA are shown in Fig. 21. We also present in Fig. 21 the results of our calculations for a potential we denote as HM3′.[18] The dashed lines are the results for the standard model and the solid lines include the relativistic correction. The generally accepted values for the binding energy and saturation density of nuclear matter correspond to values inside the rectangle in Fig. 21.

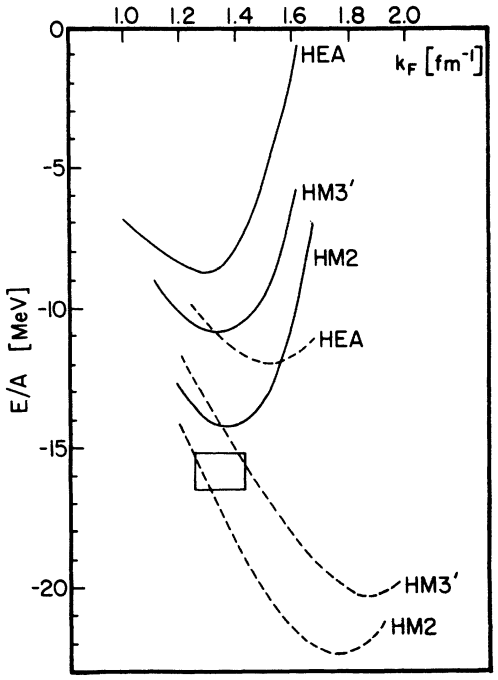

FIG. 21. The dashed lines labeled HEA, HM2, and HM3′ denote the saturation curves for the standard calculation (Ref. 1) for the potentials of Refs. 17, 9, and 18, respectively. The solid lines are the saturation curves for these potentials when calculations are made using the relativistic theory. The empirical values for the density and binding energy lie within the rectangle (Ref. 5).

As can be seen from the figure, *the relativistic correction takes one off the Coester line*. Further, the interaction HM2 gives saturation at the correct density and with a binding energy per particle of 14.2 MeV. (An additional 1 or 2 MeV binding may arise as the contribution of three-body cluster terms.[5] Such calculations have not been made for interactions with weak tensor forces such as HM2.) We find it gratifying that a generally satisfactory result is obtained with HM2 since there is a body of evidence[6-8] that favors strong ρ-meson tensor coupling and relatively weak tensor interaction, both characteristics of HM2.

IX. CONCLUSION

While the relativistic quasipotential method has been extensively applied in the study of nucleon-nucleon scattering, there have been relatively few applications of this method to bound state problems. Indeed, almost all applications have been in the study of the deuteron. In this work we have applied this method to study the properties of nuclear matter and have found large corrections to the nonrelativistic theory.

One should note that only a limited set of matrix elements of the quasipotential U are determined in the study of nucleon-nucleon scattering. (In the notation used here only the matrix elements of U^{++++} are relevant in the analysis of scattering data if one uses a Green's function such as g^{++} which restricts the intermediate nucleons to positive energy spinor states.) In the study of nuclear matter other matrix elements of U come into play and these elements are responsible for our success in providing a more satisfactory description of the saturation properties of nuclear matter.

Clearly, further studies are called for. In particular we plan to study the properties of finite nuclei. Almost all calculations of finite nuclei using the nonrelativistic Brueckner-Hartree-Fock theory yield too small radii and/or insufficient binding. We will investigate whether the use of our relativistic theory will lead to an improved description. Further, we can study the spin-orbit splitting in the finite system as well as the role of three-body forces. It is clear that if one constructs a description of nuclear structure based upon the use of only positive energy Dirac spinors or Pauli spinors to describe the states of the nucleon, one will need significant three-body forces due to the relativistic effects considered here.

This work was supported in part by the National Science Foundation and the PSC-BHE Award program of the City University of New York.

APPENDIX A

In this appendix we discuss an alternate representation of $\Sigma(\vec{p})$. We may write a general form

$$\mathbf{\Sigma}(\vec{p}) = A(\vec{p}) + B(\vec{p})\gamma^0 + \frac{\vec{\gamma}\cdot\vec{p}}{m} C(\vec{p}). \tag{A1}$$

Recalling the definitions of $\Sigma^{++}(\vec{p})$, $\Sigma^{-+}(\vec{p})$, and $\Sigma^{--}(\vec{p})$ we have

$$\Sigma^{++}_{ss'}(\vec{p}) = \delta_{ss'}\left[A(\vec{p}) + \frac{E(\vec{p})}{m} B(\vec{p}) + \frac{\vec{p}^2}{m^2} C(\vec{p})\right], \tag{A2}$$

$$\Sigma^{-+}_{ss'}(\vec{p}) = \langle s|\vec{\sigma}\cdot\hat{\vec{p}}|s'\rangle \frac{|\vec{p}|}{m}[C(\vec{p}) - A(\vec{p})], \tag{A3}$$

and

$$\Sigma^{--}_{ss'}(\vec{p}) = \delta_{ss'}\left[-A(\vec{p}) + \frac{E(\vec{p})}{m} B(\vec{p}) - \frac{\vec{p}^2}{m^2} C(\vec{p})\right]. \tag{A4}$$

Thus the quantity $\Sigma^{-+}(\vec{p}) \equiv \Sigma^{-+}_{1/2\,1/2}(\vec{p})$ is given by

$$\Sigma^{-+}(\vec{p}) = \frac{|\vec{p}|}{m}[C(\vec{p}) - A(\vec{p})]; \quad \vec{p} = p\hat{z}. \tag{A5}$$

In obtaining these results we have used the relations

$$\bar{u}^{(s')}(\vec{p})u^{(s)}(\vec{p}) = \delta_{ss'}, \quad \bar{w}^{(s')}(\vec{p})w^{(s)}(\vec{p}) = -\delta_{ss'}, \tag{A6}$$

$$\bar{u}^{(s')}(\vec{p})\gamma^0 u^{(s)}(\vec{p}) = \frac{E(\vec{p})}{m}\delta_{ss'},$$
$$\bar{w}^{(s')}(\vec{p})\gamma^0 w^{(s)}(\vec{p}) = \frac{E(\vec{p})}{m}\delta_{ss'}, \tag{A7}$$

$$\bar{u}^{(s')}(\vec{p})\vec{\gamma}\cdot\vec{p}\,u^{(s)}(\vec{p}) = \frac{\vec{p}^2}{m^2}\delta_{ss'},$$
$$\bar{w}^{(s')}(\vec{p})\vec{\gamma}\cdot\vec{p}\,w^{(s)}(\vec{p}) = -\frac{\vec{p}^2}{m^2}\delta_{ss'}, \tag{A8}$$

$$\bar{u}^{(s')}(\vec{p})w^{(s)}(\vec{p}) = -\left\langle s'\left|\frac{\vec{\sigma}\cdot\vec{p}}{m}\right|s\right\rangle, \tag{A9}$$

$$\bar{u}^{(s')}(\vec{p})\gamma^0 w^{(s)}(\vec{p}) = 0, \tag{A10}$$

and

$$\bar{u}^{(s')}(\vec{p})\vec{\gamma}\cdot\vec{p}\,w^{(s)}(\vec{p}) = \langle s'|\sigma\cdot\vec{p}\,|s\rangle. \tag{A11}$$

We may solve for A, B, and C to obtain

$$A(\vec{p}) = \left[\frac{m}{E(\vec{p})}\right]^2\left[\frac{\Sigma^{++}(\vec{p}) - \Sigma^{--}(\vec{p})}{2} - \frac{|\vec{p}|}{m}\Sigma^{-+}(\vec{p})\right], \tag{A12}$$

$$B(\vec{p}) = \frac{m}{E(\vec{p})}\left[\frac{\Sigma^{++}(\vec{p}) + \Sigma^{--}(\vec{p})}{2}\right], \tag{A13}$$

and

$$C(\vec{p}) = \left[\frac{m}{E(\vec{p})}\right]^2\left\{\frac{m}{|\vec{p}|}\Sigma^{-+}(\vec{p}) + \left[\frac{\Sigma^{++}(\vec{p}) - \Sigma^{--}(\vec{p})}{2}\right]\right\}. \tag{A14}$$

Our results for $A(\vec{p})$, $B(\vec{p})$, and $C(\vec{p})$ are shown in Fig. 22 (HM2) and Fig. 23 (HEA). As can be seen from these figures, the quantity $C(\vec{p})$ is quite small. Indeed if we neglect $C(\vec{p})$ we have

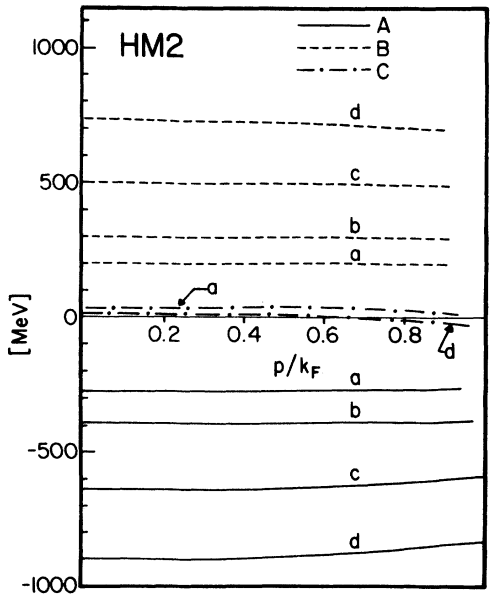

FIG. 22. The quantities A, B, and C [See Eqs. (A1)–(A14)] for the potential denoted as HM2. (a) k_F=1.2 fm^{-1}, (b) k_F=1.36 fm^{-1}, (c) k_F=1.6 fm^{-1}, and (d) k_F=1.8 fm^{-1}.

the approximate relation

$$\Sigma^{++}(\vec{p})-\Sigma^{--}(\vec{p})\simeq -2\,\frac{m}{|\vec{p}|}\,\Sigma^{-+}(\vec{p})\,. \qquad \text{(A15)}$$

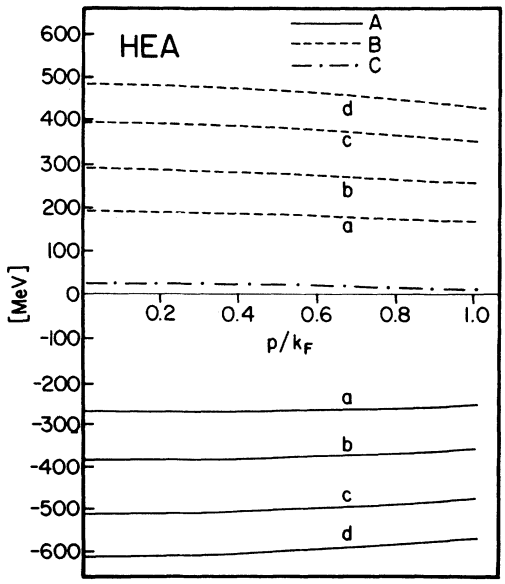

FIG. 23. The quantities A, B, and C [See Eqs. (A1)–(A14)] for the potential denoted as HEA. Only one curve is shown for C since the variation with density can not readily be exhibited in this figure. (See Fig. 22.) (a) k_F =1.2 fm^{-1}, (b) k_F=1.36 fm^{-1}, (c) k_F=1.5 fm^{-1}, and (d) k_F =1.6 fm^{-1}.

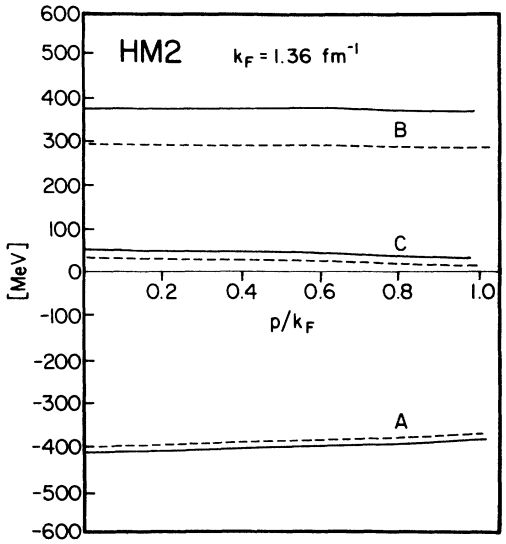

FIG. 24. The quantities A, B, and C for the potential HM2 calculated for k_F=1.36 fm^{-1}. The solid lines are the Hartree-Fock results and the dashed lines are the results when correlations are included.

The role of correlations may be seen from inspection of Fig. 24 (HM2) and Fig. 25 (HEA). Here the solid lines again represent the Hartree-Fock results and the dashed lines are the results obtained if correlations are included. It may be noted that the major correlation effects appear in the parameter $B(\vec{p})$.

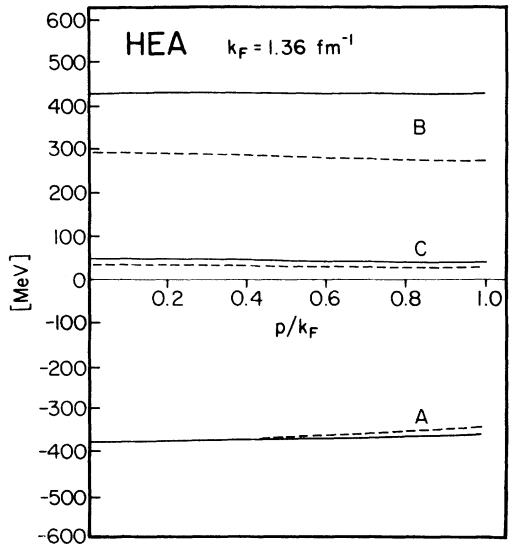

FIG. 25. The quantities A, B, and C for the potential HEA calculated for k_F=1.36 fm^{-1}. (See caption of Fig. 24.)

APPENDIX B

In this appendix, the techniques used to construct the matrix elements needed to evaluate Eqs. (2.9)–(2.11) are discussed. In general, we will extend the approach of Erkelenz[1] by transforming these matrix elements to the center-of-mass frame and helicity basis, where the contribution from individual meson exchanges are easily constructed. Each of the three cases will be considered separately.

1. $\hat{M}^{++++}$

We will discuss this case only briefly, as it corresponds very closely to the G matrix constructed in Erkelenz.[1] The matrix elements in Eq. (2.9) are Lorentz invariant so that we may transform to the center-of-mass frame

$$X_s^{++} \equiv \sum_{s'} \langle \bar{u}^{(s)}(\vec{p})\bar{u}^{(s')}(\vec{q}) \left| \hat{M}^{++++}(1-P_{12}) \right| u^{(s)}(\vec{p})u^{(s')}(\vec{q}) \rangle$$

$$= \sum_{s'} \langle \bar{u}^{(s)}(\vec{k}_c)\bar{u}^{(s')}(-\vec{k}_c) \left| \hat{M}^{++++}(1-P_{12}) \right| u^{(s)}(\vec{k}_c)u^{(s')}(-\vec{k}_c) \rangle , \tag{B1}$$

where the isospin labels are implied. Since these matrix elements are independent of s [Σ_{ss}^{++} is independent of s, see Eq. (2.1)], then

$$X_s^{++} = \tfrac{1}{4} \sum_{J T \lambda_1 \lambda_2} \frac{(2J+1)(2T+1)}{4\pi} \langle \lambda_1 \lambda_2 k_c \left| \hat{M}_{JT}^{++++}(1-P_{12}) \right| \lambda_1 \lambda_2 k_c \rangle . \tag{B2}$$

These helicity matrix elements of $\hat{M}_{JT}^{++++}$, through Eq. (1.4), are related to the helicity matrix elements of the one boson exchange potential in Ref. 1. Note that the exchange matrix elements can be constructed using the relation

$$P_{12} \left| \lambda_1 \lambda_2 J \right\rangle = (-1)^{J+1} \left| \lambda_2 \lambda_1 J \right\rangle . \tag{B3}$$

2. M^{-+++}

In this case, the transformation to the center-of-mass frame is not trivial since the matrix elements in Eq. (2.10) are not Lorentz invariant. Therefore, it is useful to reexpress the matrix elements in Eq. (2.10) in terms of Lorentz invariant ones. If we take p along the z axis, then

$$w^{(s)}(\vec{p}) = -2s \frac{|\vec{p}|}{m} u^{(s)}(\vec{p}) + \frac{E(\vec{p})}{m} v^{(-s)}(\vec{p}) . \tag{B4}$$

Therefore,

$$X_s^{-+} \equiv \sum_{s'} \langle \bar{w}^{(s)}(\vec{p})\bar{u}^{(s')}(\vec{q}) \left| \hat{M}^{-+++}(1-P_{12}) \right| u^{(s)}(\vec{p})u^{(s')}(\vec{q}) \rangle$$

$$= \sum_{s'} \left[-2s \frac{|\vec{p}|}{m} \langle \bar{u}^{(s)}(\vec{p})\bar{u}^{(s')}(\vec{q}) \left| \hat{M}^{+-++}(1-P_{12}) \right| u^{(s)}(\vec{p})u^{(s')}(\vec{q}) \rangle \right.$$

$$\left. + \frac{E(\vec{p})}{m} \langle \bar{v}^{(-s)}(\vec{p})\bar{u}^{(s')}(\vec{q}) \left| \hat{M}^{-+++}(1-P_{12}) \right| u^{(s)}(\vec{p})u^{(s')}(\vec{q}) \rangle \right] . \tag{B5}$$

We may now transform to the center-of-mass frame, but we wish to reexpress everything in terms of $u^{(s)}$ and $w^{(s)}$, so with $\vec{k}_c$ the relative momentum and using

$$v^{(s)}(\vec{k}_c) = \frac{m}{E(\vec{k}_c)} w^{(-s)}(\vec{k}_c) - 2s \frac{|\vec{k}_c| \cos\theta_{k_c}}{E(\vec{k}_c)} u^{(-s)}(\vec{k}_c) + \frac{k_c^-}{E(\vec{k}_c)} u^{(-s+1)}(\vec{k}_c) + \frac{k_c^+}{E(\vec{k}_c)} u^{(-s-1)}(\vec{k}_c) , \tag{B6}$$

where

$$k_c^{\pm} = |\vec{k}_c| \sin\theta_{k_c} e^{\pm i\phi_{k_c}} \tag{B7}$$

and taking $s = +\frac{1}{2}$, then

$$X^{\pm}_{1/2} = \sum_{s'} \left\{ \left[\frac{E(\vec{p})|\vec{k}_c|\cos\theta_{k_c}}{mE(\vec{k}_c)} - \frac{|\vec{p}|}{m} \right] \langle \bar{u}^{(1/2)}(\vec{k}_c)\bar{u}^{(s')}(-\vec{k}_c)|\hat{M}^{\pm+++}(1-P_{12})|u^{(1/2)}(\vec{k}_c)u^{(s')}(-\vec{k}_c)\rangle \right.$$

$$\left. + \frac{E(\vec{p})}{E(\vec{k}_c)} \langle \bar{w}^{(1/2)}(\vec{k}_c)\bar{u}^{(s')}(-\vec{k}_c)|\hat{M}^{\pm+++}(1-P_{12})|u^{(1/2)}(\vec{k}_c)u^{(s')}(-\vec{k}_c)\rangle \right\}. \tag{B8}$$

The first term can be constructed as in Sec. B. 1. The second term must now be expressed in the angular momentum projected helicity basis. This is also no longer trivial since this term is not independent of s. In fact,

$$\sum_{s'} \langle \bar{w}^{(s_1)}(\vec{k}_c)\bar{u}^{(s')}(-\vec{k}_c)|\hat{M}^{\pm+++}(1-P_{12})|u^{(s_2)}(\vec{k}_c)u^{(s')}(-\vec{k}_c)\rangle$$

$$= \tfrac{1}{2} \sum_{\substack{LL'JTSS' \\ \mathfrak{L}\lambda_1\lambda_2\lambda_1'\lambda_2'm}} (-)^{J+L+L'+S+S'+s_1-1/2} \frac{(2J+1)(2T+1)[(2S+1)(2S'+1)(2L+1)(2L'+1)]^{1/2}}{4\pi}$$

$$\times \langle \lambda_1'\lambda_2' k_c'|\hat{M}^{\pm+++}_{JT}(1-P_{12})|\lambda_1\lambda_2 k_c\rangle \langle L'S'J|\lambda_1'\lambda_2'J\rangle \langle \lambda_1\lambda_2 J|LSJ\rangle$$

$$\times \begin{pmatrix} L & L' & \mathfrak{L} \\ 0 & 0 & 0 \end{pmatrix} \begin{pmatrix} \frac{1}{2} & \frac{1}{2} & \mathfrak{L} \\ -s_1 & s_2 & m \end{pmatrix} \begin{Bmatrix} \mathfrak{L} & S' & S \\ J & L & L' \end{Bmatrix} \begin{Bmatrix} \mathfrak{L} & \frac{1}{2} & \frac{1}{2} \\ \frac{1}{2} & S & S' \end{Bmatrix} \left(\frac{4\pi}{(2\mathfrak{L}+1)} \right)^{1/2} Y^*_{\mathfrak{L}m}(\hat{k}_c), \tag{B9}$$

where

$$\langle LSJ|\lambda_1\lambda_2 J\rangle = \left(\frac{2L+1}{2J+1} \right)^{1/2} (L0S\lambda_1 - \lambda_2|J\lambda_1 - \lambda_2)(\tfrac{1}{2}\lambda_1\tfrac{1}{2} - \lambda_2|S\lambda_1 - \lambda_2). \tag{B10}$$

The helicity matrix elements of $\hat{M}^{\pm+++}_{JT}$ in Eq. (B9) are related through Eq. (1.4) to the helicity matrix elements of ${}^JU^{\pm+++}$ which we must now construct explicitly. As in Ref. 1,

$$\langle \lambda_1'\lambda_2' k_c'|{}^JU^{\pm+++}|\lambda_1\lambda_2 k_c\rangle = 2\pi \int_{-1}^{1} d(\cos\theta) d^J_{\lambda\lambda'}(\theta) \langle \bar{w}^{(\lambda_1')}(\vec{k}_c')\bar{u}^{(\lambda_2')}(-\vec{k}_c')|U^{\pm+++}|u^{(\lambda_1)}(\vec{k}_c)u^{(\lambda_2)}(-\vec{k}_c)\rangle, \tag{B11}$$

where $\lambda = \lambda_1 - \lambda_2$. However, now the only invariance property is

$$\langle \lambda_1'\lambda_2' k_c'|{}^JU^{\pm+++}|\lambda_1\lambda_2 k_c\rangle = -\langle -\lambda_1' - \lambda_2' k_c'|{}^JU^{\pm+++}|-\lambda_1 - \lambda_2 k_c\rangle. \tag{B12}$$

Consequently, there are now eight independent amplitudes (instead of six) and we choose the set

$$\begin{aligned}
&{}^JU_1^{\pm+++} = \langle ++k_c'|{}^JU^{\pm+++}|++k_c\rangle, \quad {}^JU_5^{\pm+++} = \langle ++k_c'|{}^JU^{\pm+++}|+-k_c\rangle, \\
&{}^JU_2^{\pm+++} = \langle ++k_c'|{}^JU^{\pm+++}|--k_c\rangle, \quad {}^JU_6^{\pm+++} = \langle +-k_c'|{}^JU^{\pm+++}|++k_c\rangle, \\
&{}^JU_3^{\pm+++} = \langle +-k_c'|{}^JU^{\pm+++}|+-k_c\rangle, \quad {}^JU_7^{\pm+++} = \langle ++k_c'|{}^JU^{\pm+++}|-+k_c\rangle, \\
&{}^JU_4^{\pm+++} = \langle +-k_c'|{}^JU^{\pm+++}|-+k_c\rangle, \quad {}^JU_8^{\pm+++} = \langle +-k_c'|{}^JU^{\pm+++}|--k_c\rangle,
\end{aligned} \tag{B13}$$

where $\lambda = \pm\frac{1}{2}$ is denoted by $\pm$. Using

$$w^{(\lambda)}(\vec{p}) \equiv v^{(-\lambda)}(-\vec{p}) = \left[\frac{E(\vec{p})+m}{2m} \right]^{1/2} \begin{pmatrix} -2\lambda|\vec{p}|/[E(\vec{p})+m] \\ 1 \end{pmatrix} |\lambda\rangle \tag{B14}$$

and Eq. (B11), the eight amplitudes in Eq. (B13) can be constructed for each type of meson exchange following the same method as Erkelenz.[1] As an example, we show, for scalar meson exchange,

$${}^JU_1^{\pm+++} = -\frac{4\pi^2 g_s^{\,2}}{m^2} \tfrac{1}{2} m(k_c' + k_c) \int_{-1}^{1} d(\cos\theta)(1+\cos\theta) \frac{1}{e} P_J(\cos\theta) \tag{B15}$$

and

$${}^JU_7^{\pm+++} = -\frac{4\pi^2 g_s^{\,2}}{m^2} \tfrac{1}{2}[-k_c' E(\vec{k}_c) + k_c E(\vec{k}_c')] \int_{-1}^{1} d(\cos\theta) \left(\frac{J}{J+1} \right)^{1/2} \frac{1}{e} [\cos\theta\, P_J(\cos\theta) - P_{J-1}(\cos\theta)], \tag{B16}$$

where θ is the angle between $\vec{k}_c$ and $\vec{k}_c'$ and $1/e$ is the meson propagator, i.e., $e = [E(\vec{k}_c') - E(\vec{k}_c)]^2 - (\vec{k}_c' - \vec{k}_c)^2$

$-\mu_s{}^2$. Again we may use Eq. (B3) to construct the exchange terms since the ket in Eq. (A9) refers to two $u^{(\lambda)}$ spinors.

3. $\hat{M}^{-+-+}$

As in Sec. B. 2, the transformation of the matrix elements in Eq. (2.11) to the center-of-mass frame is not trivial. Using Eqs. (B4), (B6), and (B7) and specializing to $s=+\frac{1}{2}$, we find

$$X_s^{--}\equiv\sum_{s'}\langle\bar{w}^{(s)}(\vec{p})\bar{u}^{(s')}(\vec{q})\,|\hat{M}^{-+-+}(1-P_{12})\,|w^{(s)}(\vec{p})u^{(s')}(\vec{q})\rangle$$

$$=\sum_{s'}\Bigg\{\left[\frac{\vec{p}}{m}-\frac{E(\vec{p})\vec{k}_c}{mE(\vec{k}_c)}\right]^2\langle\bar{u}^{(1/2)}(\vec{k}_c)\bar{u}^{(s')}(-\vec{k}_c)\,|\hat{M}^{++++}(1-P_{12})\,|u^{(1/2)}(\vec{k}_c)u^{(s')}(-\vec{k}_c)\rangle$$

$$+2\left[\frac{E^2(\vec{p})|\vec{k}_c|\cos\theta_{k_c}}{mE^2(\vec{k}_c)}-\frac{|\vec{p}|E(\vec{p})}{mE(\vec{k}_c)}\right]\langle\bar{w}^{(1/2)}(\vec{k}_c)\bar{u}^{(s')}(-\vec{k}_c)\,|\hat{M}^{-+++}(1-P_{12})\,|u^{(1/2)}(\vec{k}_c)u^{(s')}(-\vec{k}_c)\rangle$$

$$+\frac{2E^2(\vec{p})}{mE^2(\vec{k}_c)}\,|\vec{k}_c|\sin\theta_{k_c}e^{i\phi_{k_c}}\langle\bar{w}^{(1/2)}(\vec{k}_c)\bar{u}^{(s')}(-\vec{k}_c)\,|\hat{M}^{-++-}(1-P_{12})\,|u^{(-1/2)}(\vec{k}_c)u^{(s')}(-\vec{k}_c)\rangle$$

$$+\frac{E^2(\vec{p})}{E^2(\vec{k}_c)}\langle\bar{w}^{(1/2)}(\vec{k}_c)\bar{u}^{(s')}(-\vec{k}_c)\,|\hat{M}^{-+-+}(1-P_{12})\,|w^{(1/2)}(\vec{k}_c)u^{(s')}(-\vec{k}_c)\rangle\Bigg\}. \tag{B17}$$

Noting that $\sum_{ss'}\langle\bar{w}^{(s)}(\vec{k}_c)\bar{u}^{(s')}(-\vec{k}_c)\,|\hat{M}^{-++-}(1-P_{12})\,|u^{(s)}(\vec{k}_c)u^{(s')}(-\vec{k}_c)\rangle=0$ and using Eq. (B9), the third term in Eq. (B17) can be rewritten as

$$e^{i\phi_{k_c}}\sum_{s'}\langle\bar{w}^{(1/2)}(\vec{k}_c)\bar{u}^{(s')}(-\vec{k}_c)\,|\hat{M}^{-++-}(1-P_{12})\,|u^{(-1/2)}(\vec{k}_c)u^{(s')}(-\vec{k}_c)\rangle$$

$$=\tan\theta_{k_c}\sum_{s'}\langle\bar{w}^{(1/2)}(\vec{k}_c)\bar{u}^{(s')}(-\vec{k}_c)\,|\hat{M}^{-++-}(1-P_{12})\,|u^{(1/2)}(\vec{k}_c)u^{(s')}(-\vec{k}_c)\rangle \tag{B18}$$

so that Eq. (B17) becomes

$$X_{1/2}^{--}=\sum_{s'}\Bigg\{\left[\frac{\vec{p}}{m}-\frac{E(\vec{p})\vec{k}_c}{mE(\vec{k}_c)}\right]^2\langle\bar{u}^{(1/2)}(\vec{k}_c)\bar{u}^{(s')}(-\vec{k}_c)\,|\hat{M}^{++++}(1-P_{12})\,|u^{(1/2)}(\vec{k}_c)u^{(s')}(-\vec{k}_c)\rangle$$

$$+\frac{2E(\vec{p})}{mE(\vec{k}_c)}\left[\frac{E(\vec{p})|\vec{k}_c|}{E(\vec{k}_c)}\,\frac{1}{\cos\theta_{k_c}}-|\vec{p}|\right]\langle\bar{w}^{(1/2)}(\vec{k}_c)\bar{u}^{(s')}(-\vec{k}_c)\,|\hat{M}^{-++-}(1-P_{12})\,|u^{(1/2)}(\vec{k}_c)u^{(s')}(-\vec{k}_c)\rangle$$

$$+\frac{E^2(\vec{p})}{E^2(\vec{k}_c)}\langle\bar{w}^{(1/2)}(\vec{k}_c)\bar{u}^{(s')}(-\vec{k}_c)|\hat{M}^{-+-+}(1-P_{12})\,|w^{(1/2)}(\vec{k}_c)u^{(s')}(-\vec{k}_c)\rangle\Bigg\}. \tag{B19}$$

The first two terms can be evaluated as in Secs. B. 1 and B 2, respectively. Since the helicity matrix elements of $\hat{M}_{JT}^{-+-+}$ are related through Eq. (1.4) to the helicity matrix elements of ${}^JU^{-+-+}$, the last remaining problem is to construct these one boson exchange matrix elements explicitly.

To do this, we may proceed as in Sec. B 2 except that now, since both the bra and ket are a product of a $w^{(\lambda)}$ and $u^{(\lambda)}$ spinor, the exchange terms can not be obtained using the symmetry relation Eq. (B 3). They must also be constructed explicitly. With

$$\langle\lambda_1'\lambda_2'k_c'\,|{}^JU^{-+-+}(1-P_{12})\,|\lambda_1\lambda_2k_c\rangle=2\pi\int_{-1}^{1}d(\cos\theta)d^J_{\lambda\lambda'}(\theta)\langle\bar{w}^{(\lambda_1')}(\vec{k}_c')\bar{u}^{(\lambda_2')}(-\vec{k}_c')\,|{}^JU^{-+-+}(1-P_{12})\,|w^{(\lambda_1)}(\vec{k}_c)u^{(\lambda_2)}(-\vec{k}_c)\rangle \tag{B20}$$

and the symmetry property

$$\langle\lambda_1'\lambda_2'k_c'\,|{}^JU^{-+-+}(1-P_{12})\,|\lambda_1\lambda_2k_c\rangle=\langle-\lambda_1'-\lambda_2'k_c'\,|{}^JU^{-+-+}(1-P_{12})\,|-\lambda_1-\lambda_2k_c\rangle \tag{B21}$$

we again have eight independent amplitudes

$$
\begin{aligned}
&{}^{J}U_1^{++\to\to} = \langle ++k_c' |\, {}^{J}U^{++\to\to}(1-P_{12}) \,| ++k_c\rangle, \quad {}^{J}U_5^{++\to\to} = \langle ++k_c' |\, {}^{J}U^{++\to\to}(1-P_{12}) \,| +-k_c\rangle, \\
&{}^{J}U_2^{++\to\to} = \langle ++k_c' |\, {}^{J}U^{++\to\to}(1-P_{12}) \,| --k_c\rangle, \quad {}^{J}U_6^{+-\to\to} = \langle +-k_c' |\, {}^{J}U^{+-\to\to}(1-P_{12}) \,| ++k_c\rangle, \\
&{}^{J}U_3^{+-\to\to} = \langle +-k_c' |\, {}^{J}U^{+-\to\to}(1-P_{12}) \,| +-k_c\rangle, \quad {}^{J}U_7^{++\to\to} = \langle ++k_c' |\, {}^{J}U^{++\to\to}(1-P_{12}) \,| -+k_c\rangle, \\
&{}^{J}U_4^{+-\to\to} = \langle +-k_c' |\, {}^{J}U^{+-\to\to}(1-P_{12}) \,| -+k_c\rangle, \quad {}^{J}U_8^{+-\to\to} = \langle +-k_c' |\, {}^{J}U^{+-\to\to}(1-P_{12}) \,| --k_c\rangle.
\end{aligned}
\tag{B22}
$$

These eight amplitudes can be constructed for each type of meson exchange using Eq. (B14) and the method of Erkelenz.[1] As an example we show, for scalar meson exchange,

$$
{}^{J}U_1^{++\to\to} = + \frac{4\pi^2 g_s^{\,2}}{m^2} \tfrac{1}{2} \{ [k_c' k_c - E(\vec{k}_c') E(\vec{k}_c) - m^2] + (-)^J [k_c' k_c + E(\vec{k}_c') E(\vec{k}_c) - m^2] \}
$$

$$
\times \int_{-1}^{1} d(\cos\theta)(1+\cos\theta) \frac{1}{e} P_J(\cos\theta) \tag{B23}
$$

and

$$
{}^{J}U_7^{++\to\to} = \frac{4\pi^2 g_s^{\,2}}{m^2} \frac{m}{2} \{ [E(\vec{k}_c') + E(\vec{k}_c)] + (-)^J [E(\vec{k}_c) - E(\vec{k}_c')] \}
$$

$$
\times \int_{-1}^{1} d(\cos\theta) \left(\frac{J}{J+1} \right)^{1/2} \frac{1}{e} [\cos\theta P_J(\cos\theta) - P_{J-1}(\cos\theta)], \tag{B24}
$$

where again θ is the angle between $\vec{k}_c$ and $\vec{k}_c'$ and $e = [E(\vec{k}_c') - E(\vec{k}_c)]^2 - (\vec{k}_c' - \vec{k}_c)^2 - \mu_s^{\,2}$.

---

[1] K. Erkelenz, Phys. Rep. C13, 191 (1974).

[2] For a review, see G. E. Brown and A. D. Jackson, *The Nucleon-Nucleon Interaction* (North-Holland, Amsterdam, 1976).

[3] A. M. Green, Rep. Prog. Phys. 39, 1109 (1976); H. J. Weber and H. Arenhövel, Phys. Rep. C36, 277 (1978); K. Holinde and R. Machleidt, Nucl. Phys. A280, 429 (1977); K. Holinde, R. Machleidt, A. Faessler, and H. Müther, Phys. Rev. C 15, 1432 (1977); M. R. Anastasio, A. Faessler, H. Müther, K. Holinde, and R. Machleidt, *ibid.* 18, 2416 (1978).

[4] K. Holinde, Phys. Rep. (to be published).

[5] B. K. Day, Rev. Mod. Phys. 50, 495 (1978).

[6] M. R. Anastasio and G. E. Brown, Nucl. Phys. A285, 518 (1977).

[7] H. Arenhövel and W. Fabian, Nucl. Phys. A282, 397 (1977); see also, E. Lomon, Phys. Lett. 68B, 419 (1977).

[8] G. Höhler and E. Pietarinen, Nucl. Phys. B95, 210 (1975).

[9] K. Holinde and R. Machleidt, Nucl. Phys. A256, 479 (1976).

[10] J. G. Zabolitzky, Phys. Lett. 47B, 487 (1973).

[11] D. W. L. Sprung, Adv. Nucl. Phys. 5, 225 (1972); H. A. Bethe, Annu. Rev. Nucl. Sci. 21, 93 (1971); H. S. Köhler, Phys. Rep. C18, 217 (1975); J. P. Jeukenne, A. Lejeune, and C. Mahaux, *ibid.* C11, 1593 (1975).

[12] L. Celenza, L. C. Liu, and C. M. Shakin, Phys. Rev. C 11, 1593 (1975); *ibid.* 12, 721(E) (1975).

[13] C. M. Shakin and M. S. Weiss, Phys. Rev. C 15, 1911 (1977).

[14] M. R. Anastasio, L. S. Celenza, and C. M. Shakin, Brooklyn College Report No. B.C.I.N.T. 80/052/99 (unpublished).

[15] M. R. Anastasio, L. S. Celenza, and C. M. Shakin, Phys. Rev. C 23, 569 (1981).

[16] J. D. Bjorken and S. D. Drell, *Relativistic Quantum Mechanics* (McGraw-Hill, New York, 1964).

[17] K. Holinde, K. Erkelenz, and R. Alzetta, Nucl. Phys. A198, 598 (1972).

[18] The potential HM3′ refers to the potential discussed in Sec. 2.3 of Ref. 4 and whose parameters are given in Table I of that reference under the column labeled $\Lambda_\pi = 1265$.